



## Effects of solid-state fermentation with *Bacillus subtilis* LK-1 on the volatile profile, catechins composition and antioxidant activity of dark teas

Leike Xiao<sup>a,1</sup>, Chenghongwang Yang<sup>a,1</sup>, Xilu Zhang<sup>a</sup>, Yuanliang Wang<sup>a</sup>, Zongjun Li<sup>a</sup>, Yulian Chen<sup>c,\*</sup>, Zhonghua Liu<sup>b,d</sup>, Mingzhi Zhu<sup>b,d,\*</sup>, Yu Xiao<sup>a,b,\*</sup>

<sup>a</sup> College of Food Science and Technology, Hunan Agricultural University, Changsha 410128, China

<sup>b</sup> Key Laboratory of Ministry of Education for Tea Science, College of Horticulture, Hunan Agricultural University, Changsha 410128, China

<sup>c</sup> College of Animal Science and Technology, Hunan Agricultural University, Changsha 410128, China

<sup>d</sup> National Research Center of Engineering Technology for Utilization of Botanical Functional Ingredients, Hunan Agricultural University, Changsha 410128, China

### ARTICLE INFO

#### Keywords:

*Bacillus subtilis*

Dark tea

Volatile organic compounds

Solid-state fermentation

Catechins composition

Multivariate statistical analysis

### ABSTRACT

In this study, the solid-state fermentation (SSF) of dark tea was carried out using *Bacillus subtilis* LK-1, which was isolated from Fu brick tea (FBT). The effects of SSF with *B. subtilis* on volatile organic compounds (VOCs), non-volatile metabolites, and antioxidant activities of dark tea was investigated. A total of 45 VOCs were identified, primarily consisting of ketones (18), hydrocarbons (8), aldehydes (7), and alcohols (6). Following fermentation, the content of key odor active substances such as linalool,  $\beta$ -ionone, and 3,5-octadiene-2-one significantly increased, resulting in an enhanced floral and fruity aroma of dark tea. Furthermore, new flavor substances like geranyl isovalerate and decanal were produced during SSF, enriching the aroma profile of dark tea. Non-ester catechins demonstrated a drastic increase, while ester catechins remarkably decreased after SSF. Furthermore, SSF led to a slight decrease in the total polyphenols content and antioxidant activity of dark tea. There is a close relationship between VOCs and the main non-volatile metabolites during SSF. Overall, this study highlighted the great impact of SSF with *B. subtilis* on the metabolites of dark tea and provided valuable insights into the role of bacteria in shaping the metabolite profile of FBT.

### 1. Introduction

Fu brick tea (FBT), a traditional microbial post-fermented dark tea in China, has gained increasing attention due to its diverse bioactive substances and health-stimulating effects, such as anti-obesity, anti-oxidation, hypoglycemic properties, and regulation of intestinal flora (Zhu et al., 2023; Qi, Zhang, Ren, Qin, Wang, & Yang, 2023; Zhou et al., 2022). Additionally, FBT is renowned for its unique sensory characteristics. The manufacturing of FBT involves several key steps, including piling, steaming, pressing, microbial fermentation, and drying, using

primary dark tea as the raw material. Notably, microbial fermentation has been identified as a crucial process for developing the distinctive quality attributes of FBT (Chen et al., 2022; Li et al., 2020; Li et al., 2021). Microorganisms secrete various extracellular enzymes that play a crucial role in transforming tea components and generating unique metabolites in FBT (Du, Yang, Yang, & Yang, 2022; Xiao et al., 2022c). Therefore, conducting a comprehensive investigation into the role of microorganisms in the formation of FBT metabolites is essential. This research can provide valuable insights into the control and enhancement of the quality of tea products.

**Abbreviations:** BDT, *Bacillus subtilis* fermented dark tea; FBT, Fu brick tea; SSF, solid-state fermentation; VOCs, volatile organic compounds; HS-SPME-GC-MS, headspace solid-phase microextraction gas chromatography mass spectrometry; PCA, principal component analysis; PLS-DA, partial least squares-discriminant analysis; HCA, hierarchical cluster analysis; DPPH, DPPH radical scavenging activity; ABTS, ABTS radical cation scavenging activity; RP, reducing power; CHA, chelating ability; TPC, total polyphenols content; TFC, total flavonoids content; GA, gallic acid; CG, catechin gallate; C, catechin; EC, epicatechin; EGC, epigallocatechin; GCG, gallocatechin gallate; ECG, epicatechin gallate; EGCG, epigallocatechin gallate; GC, gallocatechin.

\* Corresponding authors at: College of Food Science and Technology, Hunan Agricultural University, Changsha 410128, China (Y. Xiao). Key Laboratory of Ministry of Education for Tea Science, College of Horticulture, Hunan Agricultural University, Changsha 410128, China (M. Zhu). College of Animal Science and Technology, Hunan Agricultural University, Changsha 410128, China (Y. Chen).

E-mail addresses: [chenylhn@163.com](mailto:chenylhn@163.com) (Y. Chen), [mzzhucn@hotmail.com](mailto:mzzhucn@hotmail.com) (M. Zhu), [yuxiao\\_89@163.com](mailto:yuxiao_89@163.com), [xiaoyu@hunau.edu.cn](mailto:xiaoyu@hunau.edu.cn) (Y. Xiao).

<sup>1</sup> These authors contributed equally to this work.

<https://doi.org/10.1016/j.fochx.2023.100811>

Received 18 April 2023; Received in revised form 16 July 2023; Accepted 24 July 2023

Available online 28 July 2023

2590-1575/© 2023 The Authors. Published by Elsevier Ltd. This is an open access article under the CC BY-NC-ND license (<http://creativecommons.org/licenses/by-nc-nd/4.0/>).

In recent years, various technologies, such as polymerase chain reaction-denaturing gradient gel electrophoresis (PCR-DGGE), Illumina MiSeq sequencing of ITS gene amplicons, and high-throughput Illumina MiSeq sequencing combined with quantitative polymerase chain reaction (qPCR), have been employed to explore the microbial composition and dynamic changes during the fermentation process of FBT. These studies have revealed that *Aspergillus* consistently dominates the entire FBT production process, while *Bacillus* species are particularly abundant during the flowering stage, making them the dominant bacteria in FBT fermentation (Xu, Wang, Wen, Liu, Liu, & Li, 2011; Li et al., 2019; Li et al., 2021). Recently, researchers have begun fermenting dark tea with single strains to investigate the role of these dominant microorganisms in shaping the quality of dark tea. For instance, fermenting dark tea solely with the dominant fungus *Eurotium cristatum* resulted in a significant increase in volatile organic compounds (VOCs) with a stale and fungi flower fragrance, thereby enhancing the sensory quality of dark tea (Xiao et al., 2022b). At the same time, it also led to a substantial decrease in the content of total polyphenols, flavonoids, thearubins, theaflavins, and gallate catechins (Xiao et al., 2022a). Furthermore, fermenting dark tea exclusively with *Aspergillus niger* resulted in elevated levels of  $\beta$ -ionone, 9,12-octadecadienoic acid, linalool oxides, and geraniol (Cao et al., 2018).

Notably, the previous studies mentioned above primarily focused on the investigation of fungi, particularly research on *E. cristatum* (Xiao et al., 2021b; Xiao et al., 2022a). However, bacteria also play a significant role in the microbial fermentation of FBT (Li et al., 2021), and studies have identified *Bacillus* as the dominant microorganism in FBT using culture-dependent methods and high-throughput sequencing (Xiang et al., 2022; Li et al., 2019). Several previous studies have reported a close relationship between the change in chemical constituents and *Bacillus* during FBT manufacturing through correlation analysis. *Bacillus* has been found to promote the metabolism of tea polyphenols and the transformation of caffeine, which is associated with the production of 44 metabolites in FBT (Li et al., 2019; Xia et al., 2022). Furthermore, earlier research has demonstrated that *Bacillus* species contribute to the formation of aroma characteristics in tea (Pripdeevech et al., 2014; Zhu et al., 2022). Therefore, *Bacillus* species play a crucial role in the formation of metabolites during the manufacturing of FBT. *B. subtilis*, a member of the *Bacillus* genus, has received significant attention in recent decades because it is considered a probiotic with the ability to transform food constituents. *B. subtilis* secretes highly active extracellular enzymes, such as protease, amylase, and cellulase, which may play a key role in the transformation of tea metabolites (Li & Wang, 2021). Pripdeevech et al. (2014) found that fermentation of Green Oolong tea by *B. subtilis* significantly increased the content of most major VOCs, particularly 2-pentylfuran and limonene. Xu et al. (2019) explored the effects of mixed fermentation using *B. subtilis* and *A. fumigatus* on the quality of Qingzhuang brick tea and observed a significant decrease in the content of tea polyphenols, catechins, and theabrownin after solid-state fermentation (SSF). The aforementioned research demonstrates the significant impact of *B. subtilis* fermentation on the quality of tea. However, to date, no systematic study on the metabolic characteristics of dark tea during fermentation using *B. subtilis* as a pure culture has been conducted.

In this study, a strain of *B. subtilis* LK-1, which was isolated from the microbial fermentation process during FBT manufacturing, was utilized for SSF of primary dark tea, the raw material for FBT. The objective of this study was to investigate the dynamic changes in VOCs, non-volatile components, and antioxidant activity during the fermentation process. The main aim was to elucidate the role of *B. subtilis* in the formation of metabolites in FBT. By doing so, this study aimed to provide theoretical support for understanding the involvement of bacteria in the formation of distinctive aromatic compounds and non-volatile metabolites during the fermentation process of dark tea.

## 2. Materials and methods

### 2.1. Materials and chemicals

The gallic acid (GA), gallic acid gallate (GCG), gallic acid catechin (GC), epigallocatechin (EGC), epigallocatechin gallate (EGCG), epicatechin gallate (ECG), epicatechin (EC), catechin (C), catechin gallate (CG), rutin, Folin-Ciocalteu's reagent, diammonium 2,2'-azino-bis(3-ethylbenzothiazoline-6-sulfonate) (ABTS), 2,2-diphenyl-1-picrylhydrazyl (DPPH), and ferrozine monosodium salt were supplied by Sigma-Aldrich Co. (St Louis, MO, USA). HPLC grade solvents, formic acid, and acetonitrile were provided by Fischer Scientific Co., Ltd. in Waltham, USA. All other chemicals and reagents used were of analytical grade. The *B. subtilis* LK-1 strain isolated from FBT in our laboratory was utilized as the inoculating starter for the fermentation of dark tea. The primary dark tea material was provided by Hunan Jiuyang Tea Co., Ltd. (Yiyang, China) and prepared according to the following procedure: fresh leaves  $\rightarrow$  fixation  $\rightarrow$  rolling  $\rightarrow$  piling  $\rightarrow$  drying. The related process parameters are detailed as follows: (1) fresh leaves: the raw material is one bud, three to five leaves, and the same tenderness of the leaves; (2) fixation: temperature is 220 °C–260 °C, the fixation time is 4–5 min; (3) rolling: divided into three stages of "light-heavy-light", the total time is approximately 15 min; (4) piling: piling lasting 12–18 h until the leaves color changes from dark green to yellow–brown; (5) drying: auto drying machine was used for drying the fermentation leaves at 110–150 °C for two times until the moisture content of tea leaves is below 10%.

### 2.2. Strain identification

The morphological observation and Gram staining test of strains followed the method described by Dong & Cai (2001). For bacterial identification, physiological and biochemical tests were conducted on strain LK-1 according to the guidelines provided in Bergey's Manual of Determinative Bacteriology (Buchanan & Gibbons, 1984). To perform molecular biological identification, the strain's genome was extracted, and the 16S rDNA gene was amplified using PCR with universal primers 27F and 1492R. The amplified gene was then sequenced. The obtained sequence data were submitted to the NCBI GenBank database for BLAST analysis to determine its similarity to known sequences. Multiple sequence alignment was performed using ClusterX software, and the phylogenetic tree was constructed using MEGA-X software.

### 2.3. Preparation of starter inoculum

*B. subtilis* was inoculated into 50 mL of lysogeny broth (LB) medium and cultured at 37 °C for 24 h. Subsequently, 3 mL of the activated first generation was transferred into 150 mL of fresh LB broth medium and incubated for 12 h at 37 °C. The bacterial cells were harvested by centrifugation at 8000 rpm for 5 min at 4 °C and washed twice with sterilized physiological saline. The cells were then resuspended in sterilized physiological saline to achieve a concentration of  $10^8$  cells/mL.

### 2.4. Solid-state fermentation of dark tea

The preparation of fermented dark tea with *B. subtilis* involved the following steps: 20 g of primary dark tea were placed in flasks and sprayed with 12 mL of pure water. The flasks were then sterilized at 121 °C for 20 min. After the flasks cooled down to 25 °C, 4 mL of *B. subtilis* suspension was added to the dark tea leaves as a seeding culture. The flasks containing the dark tea and *B. subtilis* were placed in a microbiological incubator set to 37 °C. Sampling was conducted at various fermentation stages: initial stage (2 days, BDT2), middle stage (4 days, BDT4), and final fermentation stages (6 days, DT4; 8 days, BDT8). Dark tea sampled on day 0 (BDT0) was used as a control for comparison. The collected dark tea samples were freeze-dried and ground into powder form. The tea powders were screened through a 40-

mesh filter and stored at  $-20\text{ }^{\circ}\text{C}$  for further analysis.

## 2.5. Analysis of volatile metabolites by HS-SPME-GC-MS

Headspace solid phase microextraction was employed to extract VOCs from the *B. subtilis* fermented dark tea (BDT) samples. The detailed method was carried out as follows: In a headspace vial with a capacity of 20 mL and equipped with a magnetic stirrer, 0.5 g of BDT sample, 0.5 g of sodium chloride, 10  $\mu\text{L}$  of ethyl caprate (8.64 mg/L) as an internal standard solution, and 5 mL of boiled ultra-pure water were combined. The top of the glass bottle was sealed with a silicon diaphragm to create a sealed headspace environment. The headspace glass bottle was then heated to  $80\text{ }^{\circ}\text{C}$ , and the tea sample was stirred at a speed of 600 rpm using the magnetic stirrer. After a 10 min pre-balance period, a 50/30  $\mu\text{m}$  DVB/CAR/PDMS fiber from American Supelco was inserted into the headspace vial to extract the VOCs. The extraction process lasted for 50 min. Subsequently, the fiber was desorbed for five minutes at the injection port of the GC-MS, operating in splitless injection mode at  $250\text{ }^{\circ}\text{C}$ .

For the separation of VOCs, a  $30\text{ m} \times 0.25\text{ mm} \times 0.25\text{ }\mu\text{m}$  HP-5MS capillary column from Agilent (USA) was used. The gas chromatography-mass spectrometry (GC-MS) analysis of VOCs was performed using the Agilent 7000D system. The column temperature program was as follows: The initial temperature was set at  $40\text{ }^{\circ}\text{C}$  and maintained for 3 min. Subsequently, it increased to  $80\text{ }^{\circ}\text{C}$  at a rate of  $2\text{ }^{\circ}\text{C}/\text{min}$ , followed by an increase to  $90\text{ }^{\circ}\text{C}$  at the same rate. Subsequently, the temperature was further increased to  $150\text{ }^{\circ}\text{C}$  at a rate of  $3\text{ }^{\circ}\text{C}/\text{min}$ , then to  $180\text{ }^{\circ}\text{C}$  at  $5\text{ }^{\circ}\text{C}/\text{min}$ , and finally to  $230\text{ }^{\circ}\text{C}$  at  $15\text{ }^{\circ}\text{C}/\text{min}$ . The final temperature of  $230\text{ }^{\circ}\text{C}$  was held for 2 min. The mass spectrometry was performed using the electron impact ionization mode with the MS ion source temperature set to  $230\text{ }^{\circ}\text{C}$ . The electron energy used was 70 eV, and the mass spectrum scanning range was set from 35 to 400  $m/z$ . To calculate the retention index (RI) for each peak, the retention time (RT) of *n*-alkanes (C6 ~ C21) under the same GC-MS conditions was utilized. The identification of VOCs was accomplished by comparing the calculated RI values and the mass spectra of all detected metabolites with those present in the NIST 17 library. For quantification of VOCs, the peak area ratio of VOCs to the internal standard ethyl caprate was multiplied by the concentration of ethyl caprate.

## 2.6. Analysis of relative odor activity value

The relative odor activity value (ROAV) is a method used to identify key volatile compounds in samples, with a range from 0 to 100. The calculation of ROAV is performed using the following formula:  $\text{ROAV}_i = 100 \times (\text{OAV}_i/\text{OAV}_{\text{max}})$ . The calculation formula for the odor activity value (OAV) is as follows:  $\text{OAV}_i = C_i/\text{OT}_i$ , where  $C_i$  represents the concentration of volatile compounds in the sample, and  $\text{OT}_i$  represents the odor threshold in water (Zhu, Chen, Chen, Chen, & Deng, 2020). The odor threshold values can be obtained from previous reports (Xu et al., 2022; Xiao et al., 2022c). VOCs with an ROAV value greater than or equal to 1 are considered key volatile compounds. VOCs with an ROAV value ranging from 0.1 to <1 have a modifying effect on the overall flavor of the sample (Su, He, Zhou, Li, & Zhou, 2022).

## 2.7. Determination of major chemical composition changes in dark teas during SSF

A total of 1 g of ground BDT sample was transferred to a conical flask and mixed with 40 mL of distilled water. The mixture was then extracted in a  $95\text{ }^{\circ}\text{C}$  water bath for 30 min with intermittent shaking every 5 min. To obtain the supernatant, the extracted mixture was subjected to centrifugation using a centrifuge (3-18R, Hunan Hengnuo Instrument Equipment Co., Ltd., China) at 10,000 rpm for 15 min at  $4\text{ }^{\circ}\text{C}$ . The resulting supernatant was adjusted to a final volume of 50 mL and stored in a refrigerator at  $-20\text{ }^{\circ}\text{C}$  for further analysis. The concentration of tea

polyphenols was measured using the Folin-Ciocalteu colorimetric method, as described by Xiao et al. (2021a). The data were expressed as gallic acid equivalents (GAE) in milligrams per gram (mg/g) of dried weight tea. The determination method for total flavonoids concentration followed the protocol outlined by Xiao et al. (2022a). The concentration was reported as rutin equivalents per gram of dried tea sample (mg RE/g d.w.).

The quantitative analysis of gallic acid (GA) and catechins was performed using the Agilent 1260 HPLC system from Agilent Technologies, USA. The tea liquids obtained previously were filtered using a 0.22  $\mu\text{m}$  PVDF membrane syringe filter. Then, a 10  $\mu\text{L}$  sample was injected onto an Agilent C18 reverse-phase column (ZORBAX SB-C18,  $4.6 \times 250\text{ mm}$ ) packed with 5  $\mu\text{m}$  particle size, which was maintained at a temperature of  $30\text{ }^{\circ}\text{C}$ . The HPLC system utilized Eluent A (acetonitrile) and Eluent B (0.1% formic acid in ultrapure water) as the mobile phases. The flow rate was set at 0.8 mL/min. The gradient elution program was presented as follows: from 0 to 40 min, the mobile phase composition changed from 90% to 65% B, and from 40 to 42 min, it returned to 90% B. To measure the analytes, a G7111A Quat Pump, AutoSampler, G7114A VWD detector, and detection at a wavelength of 280 nm were employed. By comparing the absorption spectra and retention times of the target catechins and GA with those of reference substances, the identification of these compounds was achieved. The results of the analysis were expressed as milligrams per 100 g of dried dark tea.

## 2.8. Evaluation of antioxidant activities

The antioxidant activities of the BDT samples were evaluated using several assays with different mechanisms. Following the method described in our previous study (Chen et al., 2020), the determination of reducing power (RP), DPPH radical scavenging activity (DPPH), and ABTS radical cation scavenging activity (ABTS) were conducted. The calibration curve was constructed using various concentrations of vitamin C. The results were expressed in milligrams of vitamin C equivalents per gram of dry weight dark tea flour (mg VCE/g d.w.). The chelating ability (CHA) of ferrous ions was assessed using the method previously published by Xiao et al. (2015). The calibration curve was constructed using ethylenediaminetetraacetic acid disodium salt (EDTA-2Na) solution at various concentrations. The results were expressed as milligrams of EDTA-2Na equivalents per gram of dry weight dark tea flour (mg EDTA-2Na equivalent/g d.w.).

## 2.9. Statistical analysis

The data were presented as mean  $\pm$  standard deviation, and each measurement was performed at least three times. Statistical significance ( $p < 0.05$ ) was determined using SPSS 26.0 software (Chicago, IL, USA) through single-factor ANOVA testing or independent sample *t*-tests. To analyze the correlations among the results in BDT, Pearson correlation analysis was conducted using SPSS 26.0 software. The correlations were visualized using Origin 2021. For data analysis, SIMCA 14.1 software was employed to create primary component analysis (PCA), hierarchical cluster analysis (HCA), and partial least-squares discriminant analysis (PLS-DA) models. These models were used to examine the distribution of VOCs and antioxidant activity in dark tea. The graphical display and creation of hot charts were performed using Origin 2021 (OriginLab Corporation, MA, USA) and TBtools version 1.108, respectively.

## 3. Results and discussion

### 3.1. Strain identification

The colony morphology of LK-1 strain is depicted in Fig. 1A. The colonies appeared gray, approximately circular, opaque, slightly flattened on the surface, and exhibited saw-shaped edges. Clear concentric rings were observed, which are consistent with the morphological

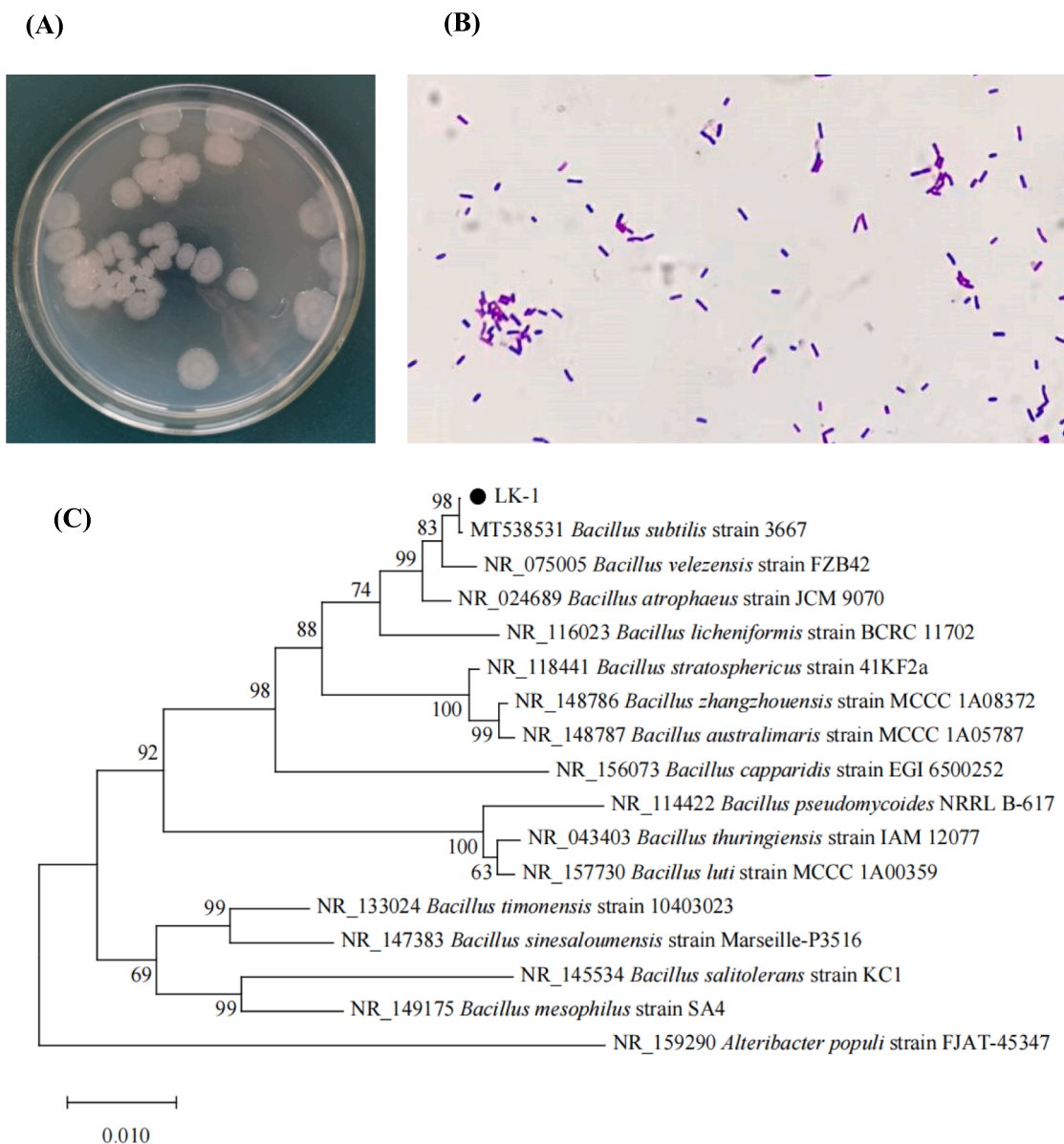


Fig. 1. (A) Colony morphology of LK-1 strain inoculated on LB medium for 12 h, (B) Gram staining diagram of strain LK-1, (C) PCR Phylogenetic tree of the 16S rDNA from strain LK-1.

characteristics of *B. subtilis* reported in previous studies (Tasaki, Nakayama, & Shoji, 2017). The gram-staining result of the strain was positive (Fig. 1B). Microscopically, the strain exhibited a rod-shaped morphology with blunt and round ends. The cells did not show significant swelling. The results of physiological and biochemical identification for strain LK-1 are presented in Table S1. The strain did not liquefy gelatin but could utilize propionate. It tested positive for the catalase and methyl red tests, while the Voges-Proskauer (V-P) test yielded a negative result. Additionally, strain LK-1 demonstrated the ability to utilize various carbohydrates such as glucose, xylose, and mannitol, but it was unable to ferment fructose. These biochemical characteristics align with the identification criteria for *B. subtilis*. Further analysis involved sequencing the 16S rDNA gene of the LK-1 strain and comparing it with sequences in the NCBI GenBank database. The comparison revealed a high similarity of 99% between the 16S rDNA gene sequence of LK-1 and *B. subtilis*. A phylogenetic tree was constructed using 16 sequences with high similarity, as shown in Fig. 1C. LK-1 and *B. subtilis* strains clustered together, indicating a close genetic

relationship. Therefore, LK-1 was identified as *B. subtilis*.

### 3.2. Analysis of VOCs during SSF with *B. Subtilis*

#### 3.2.1. Qualitative and quantitative analysis of VOCs by GC-MS

The typical total ion chromatogram of VOCs is depicted in Fig. 2A, while Table 1 provides qualitative and quantitative analysis of the identified VOCs. A total of 45 VOCs were identified using GC-MS, including aldehydes (7), esters (2), alcohols (6), ketones (18), hydrocarbons (8), heterocyclics (3), and lactones (1). The relative proportion of these categorized VOCs is illustrated in Fig. 2B, with ketones (40%), hydrocarbons (17.78%), aldehydes (15.56%), and alcohols (13.33%) constituting a significant portion. This result agrees with previous investigations of dark tea (Shi, Zhu, Zhang, Lin, & Lv, 2019). To analyze shared and distinctive traits among each sample, a Venn diagram (Fig. 2C) was employed. It reveals that there are 29 VOCs shared by all groups, and the number of VOCs increases with the progression of fermentation days. In Fig. 2D, the total content of each volatile category

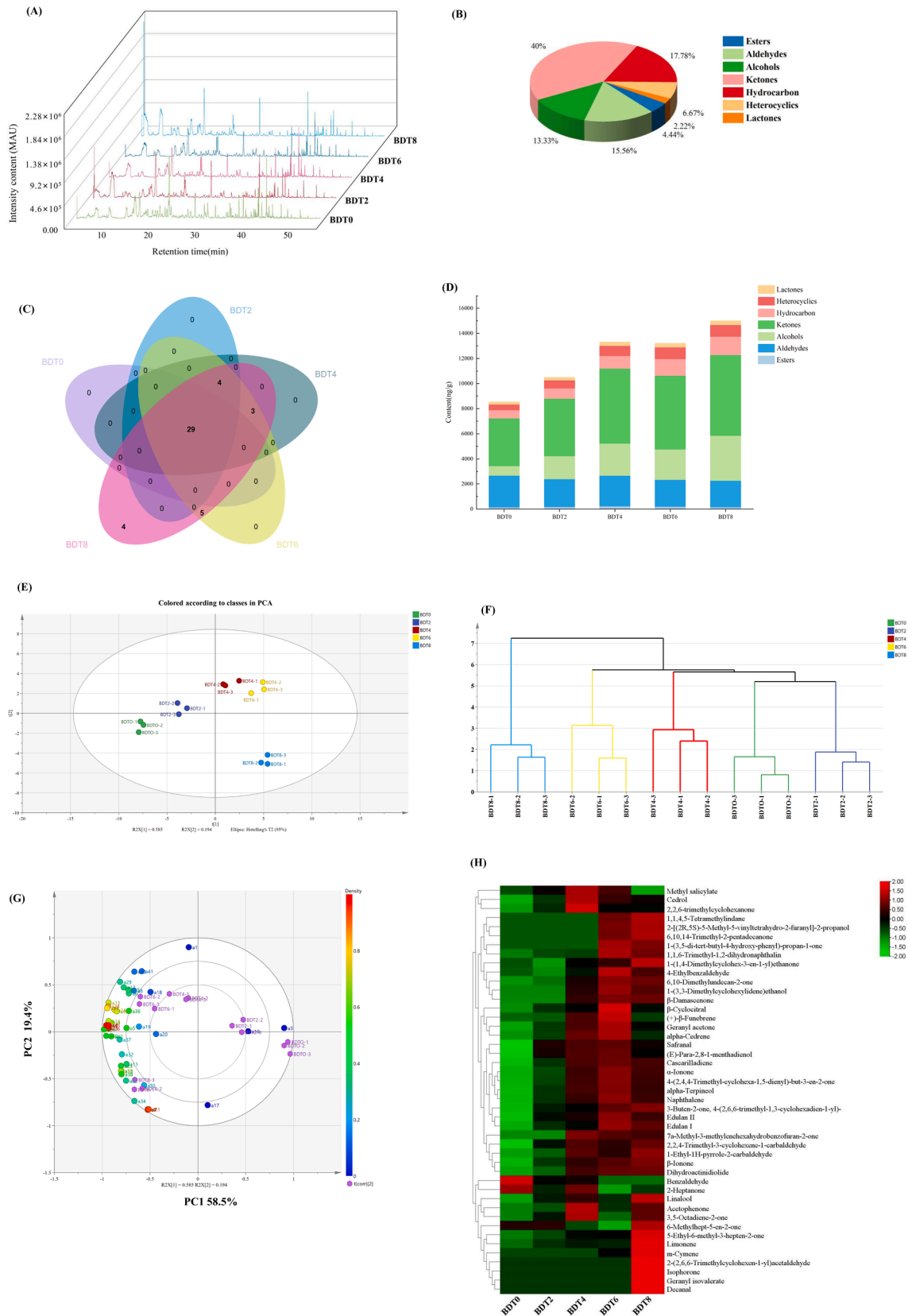


**Fig. 2.** (A) GC-MS total ion chromatograms, (B) Venn diagram, (C) Classification of all VOCs, (D) Changes in the content of classified volatiles, (E) Principal component analysis, (F) Hierarchical cluster analysis, (G) Loading plot based on the signal intensity of VOCs of dark teas at different fermentation stages. (H) Heatmap analysis of all VOCs detected by GC-MS during the fermentation of dark tea by *B. subtilis*.

**Table 1**  
Concentration of volatile compounds among dark teas fermented by *B. subtilis* by GC-MS.

No	Compounds	CAS	RI <sup>a</sup> / RI <sup>b</sup>	Identification <sup>c</sup>	Odor description	Content (ng/g)					Thresholds (ng/g)	ROAV				
						BDT0	BDT2	BDT4	BDT6	BDT8		BDT0	BDT2	BDT4	BDT6	BDT8
<b>Esters</b>																
a1	Methyl salicylate	119-36-8	1187/ 1192	MS,RI	Almond, Caramel, Peppermint, Sharp	144.77 ± 16.59c	173.18 ± 30.43b	218.98 ± 16.68a	191.74 ± 13.74a	118.26 ± 13.47c	40	0.15	0.02	0.02	0.01	0.01
a2	Geranyl isovalerate	109-20-6	1596/ 1606	MS,RI	Apple, Fruit, Rose	n.d.	n.d.	n.d.	n.d.	31.70 ± 4.5	n.f.	-	-	-	-	-
<b>Aldehydes</b>																
a3	Benzaldehyde	100-52-7	957/ 962	MS,RI	Bitter Almond, Burnt Sugar, Cherry, Malt, Roasted Pepper	1899.22 ± 7.31a	1228.25 ± 117.49b	1302.68 ± 77.91b	868.38 ± 31.37c	859.01 ± 5.39c	350	0.22	0.06	0.05	0.04	0.02
a4	2,2,4-Trimethyl-3-cyclohexene-1- carbaldehyde	127128-60-3	1137/ 1138	MS,RI	-	n.d.	100.57 ± 7.75c	149.81 ± 11.87b	131.47 ± 6.3b	160.19 ± 14.22a	n.f.	-	-	-	-	-
a5	4-Ethylbenzaldehyde	4748-78-1	1177/ 1180	MS,RI	-	127.26 ± 5.08c	118.47 ± 7.4c	144.36 ± 10.21b	186.96 ± 11.44a	165.04 ± 35.65a	n.f.	-	-	-	-	-
a6	Safranal	116-26-7	1193/ 1201	MS,RI	Saffron	268.24 ± 26.68b	492.17 ± 53.86a	535.25 ± 16.75a	550.6 ± 47.83a	477.88 ± 82.15a	3	3.61	2.87	2.34	2.65	1.48
a7	Decanal	112-31-2	1204/ 1206	MS,RI	Floral, Fried, Orange Peel, Penetrating, Tallow	n.d.	n.d.	n.d.	n.d.	41.45 ± 5.99	0.1	-	-	-	-	3.86
a8	β-Cyclocitral	432-25-7	1217/ 1220	MS,RI	Mint-like	238.22 ± 59.76b	284.86 ± 17.75b	315.64 ± 31.73b	418.02 ± 65.18a	305.45 ± 31.23b	3	3.20	1.66	1.38	2.01	0.95
a9	2-(2,6,6-Trimethylcyclohexen-1-yl) acetaldehyde	472-66-2	1264/ 1254	MS,RI	-	n.d.	n.d.	n.d.	n.d.	114.73 ± 6.96	n.f.	-	-	-	-	-
<b>Alcohols</b>																
a10	2-[(2R,5S)-5-Methyl-5- vinyltetrahydro-2-furanyl]-2-propanol	5989-33-3	1067/ 1074	MS,RI	Floral	n.d.	n.d.	n.d.	346.92 ± 34.09a	423.92 ± 44.62a	n.f.	-	-	-	-	-
a11	Linalool	78-70-6	1096/ 1099	MS,RI	Coriander, Floral, Lavender, Lemon, Rose	477.12 ± 46.2d	1259.62 ± 48.81c	1677.78 ± 177.23b	1133.73 ± 56.93c	2363.71 ± ± 291.7a	0.22	87.47	100.00	100.00	74.51	100.00
a12	(E)-Para-2,8-1-menthadienol	7212-40-0	1108/ 1123	MS,RI	-	n.d.	72.08 ± 9.38a	90.5 ± 19.07a	97.54 ± 20.58a	67.14 ± 6.69b	n.f.	-	-	-	-	-
a13	alpha-Terpineol	98-55-5	1184/ 1189	MS,RI	Pleasant, floral	170.03 ± 34.88d	325.88 ± 56.29c	468.88 ± 23.68a	529.27 ± 13.78a	451.48 ± 16.28b	86	0.08	0.07	0.07	0.09	0.05
a14	1-(3,3-Dimethylcyclohexylidene) ethanol	26532-23-0	1227/ 1225	MS,RI	-	n.d.	n.d.	54.37 ± 1.39c	88.32 ± 5.32a	69.57 ± 5.23b	n.f.	-	-	-	-	-
a15	Cedrol	77-53-2	1601/ 1598	MS,RI	Cedarwood, woody, dry, sweet, soft	115.43 ± 7.74d	170.15 ± 6.02c	272.42 ± 12.66a	221.17 ± 13.95b	203.46 ± 39.97b	1	4.66	2.97	3.57	3.20	1.89
<b>Ketones</b>																
a16	2-Heptanone	110-43-0	888/ 891	MS,RI	Blue Cheese, Fruit, Green, Nut, Spice	1030.41 ± 121.95a	864.29 ± 104.16a	997.62 ± 106.73a	756.34 ± 8.62b	845.06 ± 133.62a	65	0.64	0.23	0.20	0.17	0.12
a17	6-Methylhept-5-en-2-one	110-93-0	985/ 986	MS,RI	Citrus, Mushroom, Pepper, Rubber, Strawberry	768.36 ± 91.24a	772.92 ± 143.61a	656.57 ± 48.26b	571.1 ± 54.88c	894.34 ± 56.99a	68	0.46	0.20	0.13	0.12	0.12
a18	2,2,6-trimethylcyclohexanone	2408-37-9	1028/ 1036	MS,RI	Floral	141.58 ± 17.37b	176.56 ± 11.25b	256.18 ± 44.29a	192.85 ± 35.39b	190.08 ± 19.99b	100	0.06	0.03	0.03	0.03	0.02
a19	Acetophenone	98-86-2	1060/ 1065	MS,RI	Almonds, Flower, Meat, Must	221.5 ± 15.85b	239.22 ± 25.68b	351.07 ± 5.24a	254.82 ± 17.59b	317.74 ± 24.62a	65	0.14	0.06	0.07	0.06	0.05
a20	3,5-Octadiene-2-one	38284-27-4	1089/ 1091	MS,RI	Fruit, Fat, Mushroom- like	182.09 ± 20.93	227.43 ± 14.87	302.6 ± 39.72	192.2 ± 6.43	273.74 ± 31.25	0.15	48.96	26.48	26.45	18.53	16.99
a21	Isophorone	78-59-1	1113/ 1124	MS,RI	Sweet, Fruit	n.d.	n.d.	n.d.	n.d.	78.39 ± 14.32	11	-	-	-	-	0.07
a22	5-Ethyl-6-methyl-3-hepten-2-one	57283-79-1	1144/ 1144	MS,RI	-	195.95 ± 22.94c	217.09 ± 27.28b	245.81 ± 23.93b	250.5 ± 29.82b	338.7 ± 23.76a	n.f.	-	-	-	-	-

(continued on next page)

Table 1 (continued)

No	Compounds	CAS	RI <sup>a</sup> / RI <sup>b</sup>	Identification <sup>c</sup>	Odor description	Content (ng/g)					Thresholds (ng/g)	ROAV				
						BDT0	BDT2	BDT4	BDT6	BDT8		BDT0	BDT2	BDT4	BDT6	BDT8
a23	1-(1,4-Dimethylcyclohex-3-en-1-yl) ethanone	43219-68-7	1150/ 1149	MS,RI	Fruit	164.82 ± 7.22c	145.95 ± 6.04d	192.99 ± 26.28b	205.82 ± 21.64b	243.39 ± 7.09a	n.f.	-	-	-	-	-
a24	7a-Methyl-3-methylenehexahydrobenzofuran-2-one	67498-53-7	1300/ 1302	MS,RI	-	n.d.	n.d.	118.77 ± 8.2a	103.12 ± 2.83b	94.34 ± 7.34b	n.f.	-	-	-	-	-
a25	β-Damascenone	23726-93-4	1382/ 1386	MS,RI	Floral, fruity, honey, cooked apples	n.d.	n.d.	46.28 ± 6.08b	63.21 ± 6.65a	59.85 ± 5.67a	n.f.	-	-	303.40	456.99	278.54
a26	6,10-Dimethylundecan-2-one	1604-34-8	1401/ 1408	MS,RI	-	38.59 ± 0.35c	46.12 ± 4.21c	77.92 ± 15.42b	101.59 ± 17.29a	96.22 ± 9.6a	n.f.	-	-	-	-	-
a27	α-Ionone	127-41-3	1424/ 1426	MS,RI	Violet, Wood	233.88 ± 39.86c	350.02 ± 25.72b	506.19 ± 50.06a	583.73 ± 43.17a	514.57 ± 35.33a	3.7	2.55	1.65	1.79	2.28	1.29
a28	4-(2,4,4-Trimethyl-cyclohexa-1,5-dienyl)-but-3-en-2-one	1000187-51-9	1428/ 1423	MS,RI	-	209.56 ± 26.08c	356.87 ± 13.3b	541.73 ± 58.83a	620.65 ± 56.3a	532.48 ± 50.79a	n.f.	-	-	-	-	-
a29	Geranyl acetone	3796-70-1	1449/ 1453	MS,RI	Fruit	107.77 ± 4.24d	202.3 ± 8.38c	325.2 ± 42.97b	398.16 ± 21.02a	249.87 ± 45.4c	60	0.07	0.06	0.07	0.10	0.04
a30	3-Buten-2-one, 4-(2,6,6-trimethyl-1,3-cyclohexadien-1-yl)-	1203-08-3	1479/ 1485	MS,RI	-	n.d.	73.87 ± 13.7b	89.13 ± 2.73b	127.68 ± 17.07a	140.89 ± 10.74a	n.f.	-	-	-	-	-
a31	β-Ionone	14901-07-6	1482/ 1485	MS,RI	Floral, Violet	495.89 ± 36.78d	909.94 ± 43.57c	1264.14 ± 153.54b	1383.16 ± 135.82a	1486.21 ± 47.83a	0.2	100.00	79.46	82.88	100.00	69.16
a32	1-(3,5-di-tert-butyl-4-hydroxy-phenyl)-propan-1-one	14035-34-8	1636/ 1640	MS,RI	-	n.d.	n.d.	n.d.	35.21 ± 3.5a	30.16 ± 0.6a	n.f.	-	-	-	-	-
a33	6,10,14-Trimethyl-2-pentadecanone	502-69-2	1844/ 1844	MS,RI	Jasmine-like, oily, herbal	n.d.	n.d.	n.d.	31.13 ± 1.79b	38.49 ± 3.51a	n.f.	-	-	-	-	-
Hydrocarbon																
a34	m-Cymene	535-77-3	1019/ 1023	MS,RI	Citrus	n.d.	n.d.	n.d.	98.27 ± 48.09b	364.93 ± 18.65a	n.f.	-	-	-	-	-
a35	Limonene	138-86-3	1025/ 1026	MS,RI	Citrus, lemon, orange, green, etherel	239.43 ± 19.53b	250.82 ± 23.54b	256.2 ± 21.14b	253.99 ± 19.22b	302.71 ± 22.78a	200	0.05	0.02	0.02	0.02	0.01
a36	Naphthalene	91-20-3	1172/ 1182	MS,RI	Pungent	153.13 ± 13.64b	179.95 ± 24.68a	201.22 ± 16.29a	216.93 ± 26.88a	202.58 ± 32.04a	6	1.03	0.52	0.44	0.52	0.31
a37	1,1,6-Trimethyl-1,2-dihydronaphthalin	30364-38-6	1348/ 1354	MS,RI	-	95.78 ± 19.48b	114.03 ± 11.07b	119.15 ± 11.24b	212.04 ± 36.73a	190.51 ± 28.49a	n.f.	-	-	-	-	-
a38	1,1,4,5-Tetramethylindane	16204-57-2	1352/ 1355	MS,RI	-	n.d.	n.d.	n.d.	50.34 ± 1.42b	66.17 ± 1.44a	n.f.	-	-	-	-	-
a39	Cascarilladiene	59742-39-1	1379/ 1372	MS,RI	-	n.d.	65.7 ± 11.23b	127.39 ± 1.95a	141.9 ± 17.94a	125.29 ± 17.96a	n.f.	-	-	-	-	-
a40	alpha-Cedrene	469-61-4	1406/ 1411	MS,RI	Woody, cedar, sweet, fresh	94.03 ± 4.37b	122.15 ± 6.7b	182.17 ± 34.17a	202.98 ± 29.23a	130.28 ± 25.72b	n.f.	-	-	-	-	-
a41	(+)-β-Funebrene	79120-98-2	1415/ 1414	MS,RI	-	73.05 ± 11.73b	75.7 ± 5.64b	117.14 ± 18.36a	143.36 ± 26.74a	83.26 ± 5.74b	n.f.	-	-	-	-	-
Heterocyclics																
a42	1-Ethyl-1H-pyrrole-2-carbaldehyde	2167-14-8	1044/ 1046	MS,RI	Savory	216.24 ± 3.19c	254.88 ± 17.87c	365.48 ± 23.84a	336.07 ± 19.76b	392.65 ± 42.92a	n.f.	-	-	-	-	-
a43	Edulan II	41678-30-2	1258/ 1247	MS,RI	-	109.16 ± 6.17c	135.07 ± 11.36b	140.06 ± 8.99a	155.00 ± 3.5a	145.19 ± 11.19a	n.f.	-	-	-	-	-
a44	Edulan I	41678-29-9	1310/ 1314	MS,RI	-	124.64 ± 21.82c	258.62 ± 23.49b	302.35 ± 30.88b	446.12 ± 36.06a	400.19 ± 5.46a	n.f.	-	-	-	-	-
Lactones																
a45	Dihydroactinidiolide	17092-92-1	1529/ 1532	MS,RI	Musk, coumarin	189.87 ± 33.16b	218.67 ± 20.45b	297.11 ± 8.79a	311.61 ± 10.86a	315.02 ± 18.35a	3.8	2.02	1.01	1.03	1.19	0.77

\* Odor descriptions were from FEMA database. a: Retention index of compounds on HP-5MS; b: Retention index of compounds in references; c: "MS", mass spectrum comparison using NIST17 library. "RI", retention index in agreement with literature value; 'n.f.': threshold was not found in the literature; 'n.d.': data was not detected in the sample. The threshold of volatile compounds in water referred to the literatures [Xu et al. \(2022\)](#), [Xiao et al. \(2022c\)](#).

is depicted, indicating a significant increase in the levels of ketones and alcohols after fermentation (3790.40 ng/g → 6424.52 ng/g and 762.57 ng/g → 3579.28 ng/g, respectively). These levels remain elevated until the later stage of fermentation. This finding is consistent with previous studies that found the highest content of ketones in FBT (Lv, Wu, Li, Xu, Liu, & Meng, 2014). Overall, alcohol compounds are associated with fruity and floral aromas (Yun et al., 2021), while ketone compounds are linked to woody and floral scents (Zhang et al., 2021). This suggests that *B. subtilis* contributes to the enhancement of floral and woody aromas during the SSF of dark tea. Furthermore, it is evident from Fig. 2D that the total concentration of VOCs reaches its highest level on the eighth day of fermentation.

### 3.2.2. Changes of VOCs in dark teas during SSF

The principal component analysis was employed for data visualization, as shown in Fig. 2E. Comparing the samples at different fermentation times, noticeable changes in the flavor components of dark tea can be observed. The most significant separation is observed between BDT0 and BDT6/BDT8, indicating that *B. subtilis* has a significant impact on the flavor components of dark tea during the later stages of fermentation. BDT0 and BDT2 samples are close to each other, suggesting that dark tea fermented for 0 and 2 days share similar flavor components. Hierarchical cluster analysis (HCA) also divides the dark tea samples into four groups (BDT8, BDT6, BDT4, and BDT2-BDT0) (Fig. 2F), consistent with the PCA results. Furthermore, a partial least-squares discriminant analysis (PLS-DA) model was constructed, and a loading plot (Fig. 2G) was generated to examine the contribution of various VOCs to the flavor of dark tea.

To observe the changes in VOCs during the SSF of BDT more clearly, a heatmap was constructed and the results are displayed in Fig. 2H. The heatmap represents the concentration levels of different VOCs, with red color indicating high levels and green color indicating low levels. Esters are commonly present in tea and other plants, and methyl salicylate, in particular, plays a crucial role in promoting the “mint” attribute of FBT (Li et al., 2020). In the SSF of dark tea by *B. subtilis*, the concentration of methyl salicylate initially increased, reached its maximum in the middle stage of fermentation, and gradually decreased in the later stage. This trend is consistent with previous findings in the fermentation of dark tea by *E. cristatum* (Xiao et al., 2022b). Aldehydes make up a relatively large proportion of the compounds. Benzaldehyde, which imparts floral aroma, is a key flavor compound contributing to the characteristic aroma of tea leaves (Hu et al., 2021). The content of 2,2,4-trimethyl-3-cyclohexene-1-carbaldehyde, a methyl derivative of benzaldehyde, increased, while the content of benzaldehyde significantly decreased.  $\beta$ -Cyclocitral and safranal are characteristic aroma components of dark tea, and their concentration increases after fermentation. They are primarily produced through the oxidation and degradation of  $\beta$ -carotene (Hu et al., 2021). Alcohol compounds play an important role in the formation of dark tea aroma (Ma et al., 2021). After fermentation, the content of linalool and alpha-terpineol increased, with linalool becoming the compound with the highest content. Enzymatic hydrolysis of their tea aroma precursor glycosides during SSF contributes to the production of linalool and alpha-terpineol (Zheng, Li, Xiang, & Liang, 2016). Linalool has a great contribution to the “fungus flower” aroma of FBT (Li et al., 2020; Ma et al., 2021). The rich alpha-terpineol in dark tea can release a pleasant smell similar to lilacs. Ketone compounds have the largest proportion and highest content. 6-Methylhept-5-en-2-one,  $\alpha$ -ionone,  $\beta$ -ionone, geranyl acetone, and isophorone are the main ketone compounds in dark tea, and their content significantly increases after SSF. The increase in  $\alpha$ -ionone and  $\beta$ -ionone content is associated with the degradation of carotenoids (Wang et al., 2021).  $\beta$ -Ionone can be further oxidized to 5,6-epoxy- $\beta$ -ionone, which after two reduction steps is converted to a saturated triol that undergoes intramolecular cyclization followed by an oxidation reaction to produce dihydroactinidiolide (Ho, Zheng, & Li, 2015), the content of dihydroactinidiolide increased to a maximum ( $315.02 \pm 18.35$  ng/g) on the eighth day of SSF.

Dihydroactinidiolide is detected in a variety of tea samples (Ma et al., 2021), and it imparts a musky, coumarinaceous aroma to tea, which is considered to be a key aroma in determining the quality of dark tea (Ho et al., 2015). Acetophenone, another important volatile substance, contributes to the aroma characteristics of FBT. Its increase in SSF process related to heat and humidity effect and microbial metabolism (Lv et al., 2014). Geranyl acetone and isophorone contribute to the sweetness and fruitiness of dark tea's characteristic aroma (Hu et al., 2021). M-cymene is produced in the later stages of SSF and imparts dark tea a citrus aroma. Overall, the SSF process with *B. subtilis* influences the levels of various VOCs, contributing to the formation of the distinctive aroma characteristics of dark tea.

### 3.2.3. Critical volatile compounds

It is worth noting that not all VOCs detected in dark tea samples fermented at different times contribute significantly to the flavor of dark tea. The ROAV analysis was conducted to assess the contribution of different volatiles to dark tea aroma during SSF. The ROAV values indicate the importance of key aroma active compounds, with higher scores indicating a greater contribution to the aroma qualities of dark tea (Zhu et al., 2020). Among the VOCs analyzed (Table 1), seven key VOCs with ROAV > 1 were identified in BDT8:  $\alpha$ -ionone (ROAV = 1.29), safranal (ROAV = 1.48), cedrol (ROAV = 1.89), decanal (ROAV = 3.86), 3,5-octadiene-2-one (ROAV = 16.99),  $\beta$ -ionone (ROAV = 69.16), and linalool (ROAV = 100). Linalool has the highest ROAV and contributes the most to the flavor of dark tea. Its content increases after SSF, giving dark tea a sweet and fresh floral fragrance with hints of bergamot (Su et al., 2022).  $\beta$ -Ionone is the second most important odor active substance, contributing to the floral and violet aroma of dark tea.  $\alpha$ -Ionone imparts a violet and woody aroma, consistent with previous research indicating the significant impact of ionone on tea aroma (Hu et al., 2021). 3,5-Octadiene-2-one provides a fruit aroma to dark tea and ranks third in terms of odor activity. Decanal, despite being present in low concentrations, has a high ROAV due to its low odor threshold and contributes citrus and floral aromas to dark tea. Cedrol, a sesquiterpene alcohol, imparts a sweet and soft cedarwood odor and is a representative compound of FBT (Ma et al., 2023). Safranal provides a saffron aroma to dark tea. The concentration of all these VOCs increases significantly after fermentation, enhancing the floral and fruit aroma of dark tea. VOCs with  $0.1 \leq \text{ROAV} < 1$  include  $\beta$ -cyclocitral, 2-heptanone, 6-methylhept-5-en-2-one, and naphthalene, which have a moderating effect on the aroma characteristics of dark tea.  $\beta$ -Cyclocitral and 6-methylhept-5-en-2-one increase in content during fermentation, imparting mint and citrus aromas to dark tea. On the other hand, 2-heptanone significantly decreases in content after fermentation, reducing its contribution to the blue cheese aroma of dark tea.

### 3.3. Alteration of main metabolites of dark tea during SSF

As shown in Fig. 3, the total polyphenols content decreased during SSF, and the total flavonoids content slightly increased in the middle of fermentation and decreased in the later stage. Catechins belong to flavonoid alcohols and is the main component of tea polyphenols. Catechins are divided into ester and non-ester types, which play crucial roles in the formation of tea flavor. The content changes in GA, GCG, EGCG, EGC, GC, ECG, CG, C, and EC in BDT samples during fermentation were identified and quantified by HPLC, which are listed in Table 2. The result revealed that the content of ester catechins remarkably decreased while the content of non-ester catechins greatly increased. Compared with raw dark tea (BDT0), GCG, CG, EGCG, and ECG decreased 15.3%, 10.0%, 12.4%, and 17.3% after 8 days of fermentation, respectively. However, GC, C, and EGC greatly increased 66.8%, 22.9% and 35.3%, respectively. Among them, EGCG, as one of the richest and most active gallic acid catechins, continued to decrease during fermentation, which is in line with the evolution of EGCG of dark tea fermented by *E. cristatum* (Xiao et al., 2022a). EGCG is the major



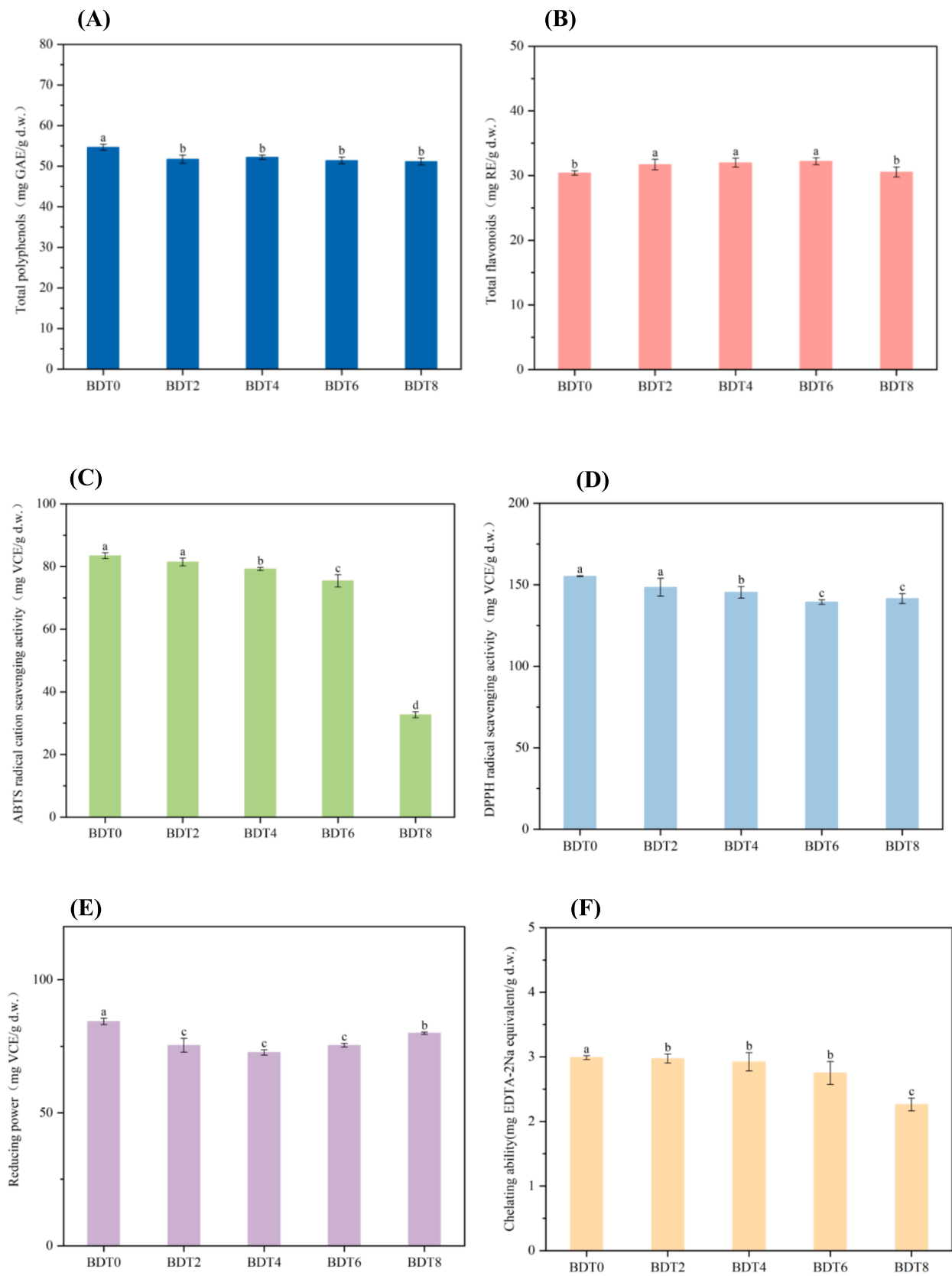


**Fig. 3.** Contents of (A) total polyphenols, (B) total flavonoids. Antioxidant activities of (C) ABTS radical cation scavenging activity, (D) DPPH radical scavenging activity, (E) reducing power, (F) chelating ability of dark tea fermented by *B. subtilis* at different times. Data were recorded as the mean value ± standard deviation of three replicates. Mean values marked by the different letters among the samples denoted significant difference ( $p < 0.05$ ).

**Table 2**  
Content of gallic acid and catechin compositions in dark tea fermented by *B. subtilis*.

Compounds	Contents (mg/100 g)				
	BDT0	BDT2	BDT4	BDT6	BDT8
GA	364.11 ± 5.44c	362.08 ± 1.98c	376.44 ± 8.21b	400.76 ± 8.36a	411.09 ± 1.82a
GC	106.58 ± 1.75c	182.02 ± 4.59a	173.12 ± 3.00b	170.79 ± 6.03b	177.80 ± 3.46a
EGC	69.55 ± 0.30b	113.39 ± 3.58a	103.99 ± 10.14a	107.72 ± 20.61a	94.10 ± 4.25a
C	344.06 ± 6.85b	381.69 ± 23.52a	377.84 ± 19.40a	419.54 ± 37.39a	422.71 ± 27.21a
EC	29.59 ± 0.83b	35.38 ± 0.24a	30.55 ± 0.47b	30.01 ± 0.46b	28.40 ± 0.25c
EGCG	156.29 ± 1.64a	151.06 ± 3.57b	150.00 ± 0.44b	136.54 ± 2.26c	136.88 ± 2.53c
GCG	342.00 ± 6.06a	315.98 ± 5.53b	302.18 ± 2.81b	290.83 ± 1.69c	289.70 ± 5.25c
ECG	124.08 ± 3.36a	122.62 ± 5.19a	109.50 ± 4.69b	104.40 ± 1.67b	102.58 ± 2.08b
CG	120.70 ± 2.31a	109.51 ± 7.52b	97.00 ± 1.14c	114.27 ± 3.26a	108.61 ± 4.37b
Non-ester catechins	549.79 ± 8.49b	712.48 ± 20.14a	685.51 ± 17.92a	728.06 ± 53.86a	723.00 ± 27.87a
Ester catechins	743.07 ± 6.38a	699.17 ± 15.28b	658.67 ± 1.36c	646.04 ± 5.70c	637.77 ± 4.09d

GA, gallic acid; GC, gallocatechin; EGC, epigallocatechin; C, catechin; EC, epicatechin; EGCG, epigallocatechin gallate; GCG, gallocatechin gallate; ECG, epicatechin gallate; CG, catechin gallate. Each tea sample was determined with three replications. Letters indicate Duncan's pairwise differences among different samples ( $p < 0.05$ ).

contributor to the bitter and astringent taste of tea infusions (Cao et al., 2019). Xiao et al. (2021b) used *E. cristatum* (MF800948) to ferment autumn green tea to reduce the content of EGCG, thereby reducing the astringency of tea. Speculating that *B. subtilis* fermented dark tea can improve the bitterness and astringency is reasonable. EGCG has a low bioavailability in the small intestine. After oral administration, only 0.1%–0.32% of EGCG can be directly bioavailable (Liu, Bruins, Ni, & Vincken, 2018). After EGCG enters the small intestine, it needs to undergo gallic acid ester hydrolysis of intestinal microbiota, C-ring cleavage and further modification of reaction products to form simple phenolic acids that are quickly absorbed by the intestinal mucosa (Xiang et al., 2018). In this study, *B. subtilis* plays a similar role to intestinal microorganisms, decomposing non-absorbable high molecular weight tea catechins into easily absorbable phenolic metabolites, and improving the biological effects related to the consumption of tea catechins. Under aerobic conditions, EGCG is hydrolyzed into EGC and gallic acid, which is the main pathway of GA biosynthesis (Tanaka, Umeki, Nagai, Shii, Matsuo, & Kouno, 2012). Indeed, as the fermentation progressed, the content of EGCG decreases, and is further metabolized, GA also increases considerably. GA has anti-inflammatory, anti-hyperlipidemic, and anti-cirrhotic effects and used in the treatment of fatty liver and diabetes (Liu et al., 2020).

Phenolic compounds are known to be the main precursors of certain volatile compounds in tea and play a crucial role in flavor development (Ayseli & Ayseli, 2016). Using GC–MS analysis, changes in VOCs content were examined, and PLS-DA analysis was conducted to identify VOCs with VIP > 1. Pearson correlation analysis was performed between these VOCs and major non-volatile metabolites (Fig. 4A). The results revealed significant positive correlations between methyl salicylate and total flavonoids, benzaldehyde and total flavonoids, EGCG, and GCG, as well as safranal and EGC, GC. On the other hand, significant negative correlations were observed between 2,2,4-trimethyl-3-cyclohexene-1-carbaldehyde and total polyphenols, GCG, 4-ethylbenzaldehyde and EGCG, ECG. Moreover, safranal showed a negative correlation with total polyphenols, while CG displayed negative correlations with 2,2,6-trimethylcyclohexanone, acetophenone, and 3,5-octadiene-2-one. These

findings suggest a close relationship between VOCs and the changes observed in these non-volatile metabolites.

### 3.4. Changes of antioxidant activity of dark tea during SSF

The antioxidant activity of dark tea samples fermented by *B. subtilis* was assessed using four different antioxidant capacity assays with distinct mechanisms (Fig. 3). The results indicated that the ABTS radical cation scavenging activity and chelating ability remained relatively stable during the early and middle stages of fermentation, retaining approximately 90.38% and 92.07% of the original antioxidant activity by the sixth day of fermentation. However, a significant decrease in ABTS radical cation scavenging activity was observed by the eighth day of fermentation. The DPPH radical scavenging activity and reducing power exhibited a slight decline throughout the fermentation process, but maintained approximately 91.14% and 94.78% of the original activity until the eighth day of fermentation. In summary, the optimal duration for maintaining the maximum antioxidant activity and enhancing the flavor of dark tea through *B. subtilis* fermentation was found to be 6 days.

Then, PCA was to examine the relationship between antioxidant activity, bioactive ingredients, and antioxidant capabilities. The PCA score plot (Fig. S1A) demonstrated clear distinctions among tea samples with different fermentation periods. The BDT4 and BDT6 sample located in the upper right quadrant of Fig. S1A was positively correlated with PC1 and PC2, suggesting a higher level of polyphenol metabolites and relatively strong antioxidant activity. To identify key contributors, a loading plot (Fig. S1B) was generated. The loading patterns of ABTS, DPPH, and CHA on PC1 indicated their association with antioxidant activity. Moreover, EGCG, ECG, GCG, TPC, CG, and EC showed higher loadings on PC1, indicating that polyphenols are effective antioxidants. The presence of polyphenols in dark tea samples of different fermentation durations is known to contribute to the variations in antioxidant capacity (Dai et al., 2015).

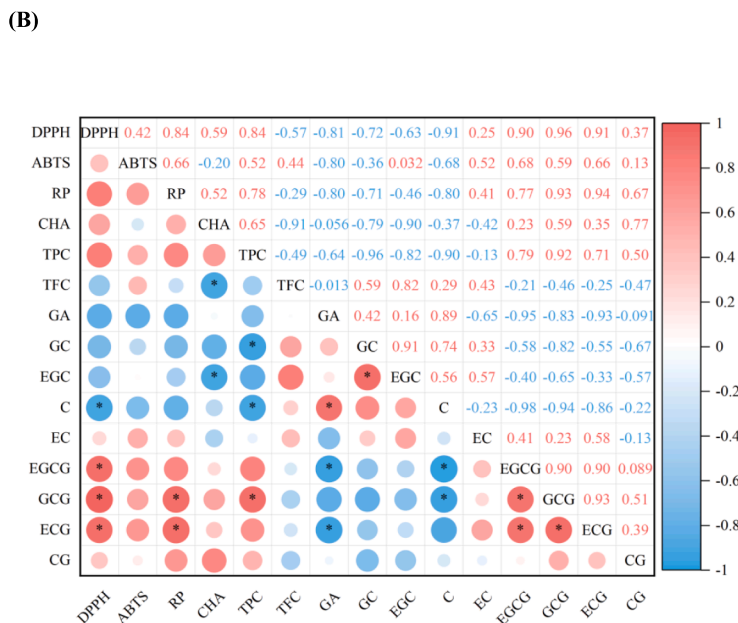
Correlation analysis was conducted to verify the relationship between antioxidant activity and polyphenols in tea products (Fig. 4B). Notably, there were significant positive correlations between EGCG, GCG, ECG, and DPPH. Similarly, GCG, ECG, and RP also exhibited significant positive correlations. The *O*-dihydroxy or trihydroxy structure, which enables chelation of metal ions and inhibition of free radical production, is one of the chemical structures responsible for the potent antioxidant activity of catechins. Among them, EGCG, with its four dihydroxy groups, is recognized as the most effective tea antioxidant (Dufresne & Farnworth, 2001). Despite the substantial decrease in EGCG and other ester-type catechins, dark tea retained its high antioxidant activity. This could be attributed to the degradation of EGCG into EGC, which possesses a high degree of hydroxylation on the B ring, resulting in great antioxidant capacity. Additionally, the degradation products of EGCG may exhibit synergistic effects with other components (e.g., ascorbic acid, vitamin E), further enhancing the antioxidant capacity.

## 4. Conclusions

The study revealed that the SSF of dark tea by *B. subtilis* LK-1 had great effects on the change of VOCs and catechins. The fermentation process led to a notable increase in the total content and abundance of VOCs, with ketones emerging as the major compounds. Several newly generated VOCs were detected in the BDT, including geranyl isovalerate and isophorone with fruity aroma, decanal with floral aroma, and m-cymene with citrus aroma, which enriched the overall aroma profile of dark tea. Key odor-active compounds such as linalool,  $\beta$ -ionone, and safranal contributed to the floral aroma of dark tea, while 3,5-octadiene 2-one and decanal imparted a fruit aroma, and cedrol and  $\alpha$ -ionone contributed to the woody aroma. The contents of these compounds significantly increased during fermentation, particularly in the later stage, indicating that *B. subtilis* fermentation enhanced the intensity of



**Fig. 4.** (A) Correlation analysis between VOCs and the main non-volatile metabolites during SSF with *B. subtilis*. (B) The correlation between the antioxidant activity of dark teas fermented by *B. subtilis* and the content of catechins, total phenols and total flavonoids. Note: the detail names of the VOCs are shown in Table 1. GA, gallic acid; GC, catechin gallate; C, catechin; EC, epicatechin; EGCG, epigallocatechin; GCG, galocatechin gallate; ECG, epicatechin gallate; EGCG, epigallocatechin gallate; GC, galocatechin; TCs, total catechins; TPC, total polyphenols; TFC, total flavonoids. DPPH, DPPH radical scavenging activity; ABTS, ABTS radical cation scavenging activity; RP, reducing power; CHA, chelating ability.



\* p<0.05

floral, fruity, and woody aromas in dark tea. The ester-type catechins in dark tea exhibited a significant decrease, while the non-ester-type catechins showed a notable increase after SSF. This shift in catechin composition may contribute to the reduction in bitterness and astringency of the tea. The antioxidant activity of dark tea was positively correlated with the levels of EGCG, GCG, and ECG, and remained high on the 6th day of fermentation. This suggests that a 6-day fermentation period using *B. subtilis* is optimal for maintaining high antioxidant activity and enhancing the flavor of dark tea. The findings demonstrate that *B. subtilis* plays a crucial role in the metabolism and transformation of both volatile and non-volatile components during the production process of dark tea. These results provide a valuable foundation for future investigations on the influence of bacteria in the quality formation of fermented dark tea.

**CRedit authorship contribution statement**

Leike Xiao: Methodology, Data curation, Validation, Writing –

original draft, Investigation. **Chenghongwang Yang:** Writing – original draft, Investigation. **Xilu Zhang:** Investigation. **Yuanliang Wang:** Resources. **Zongjun Li:** Resources. **Yulian Chen:** Formal analysis, Investigation, Conceptualization, Data curation, Methodology, Writing – original draft, Writing – review & editing. **Zhonghua Liu:** Supervision. **Mingzhi Zhu:** Project administration, Resources, Writing – review & editing. **Yu Xiao:** Project administration, Formal analysis, Methodology, Supervision, Funding acquisition, Conceptualization, Data curation, Validation, Writing – original draft, Writing – review & editing, Investigation.

**Declaration of Competing Interest**

The authors declare that they have no known competing financial interests or personal relationships that could have appeared to influence the work reported in this paper.

## Data availability

Data will be made available on request.

## Acknowledgements

The authors appreciate the financial support from the Key Technologies Research and Development Program of Hunan Province (2023NK2025), the National Key R&D Program (2022YFE0111200), the Science Research Project of Education Department of Hunan Province (No. 22C0108) and Natural Science Foundation of China (No. 32002095).

## Appendix A. Supplementary data

Supplementary data to this article can be found online at <https://doi.org/10.1016/j.fochx.2023.100811>.

## References

- Ayseli, M. T., & Ayseli, Y.I. (2016). Flavors of the future: Health benefits of flavor precursors and volatile compounds in plant foods. *Trends in Food Science & Technology*, 48, 69–77. <https://doi.org/10.1016/j.tifs.2015.11.005>
- Buchanan, R. E., & Gibbons, N. E. (1984). *Bergey's manual of determinative bacteriology* (8th (Chinese ed.). Beijing: Science Press.
- Cao, L., Guo, X., Liu, G., Song, Y., Ho, C. T., Hou, R., ... Wan, X. (2018). A comparative analysis for the volatile compounds of various Chinese dark teas using combinatory metabolomics and fungal solid-state fermentation. *Journal of Food and Drug Analysis*, 26(1), 112–123. <https://doi.org/10.1016/j.jfda.2016.11.020>
- Cao, Q. Q., Zou, C., Zhang, Y. H., Du, Q. Z., Yin, J. F., Shi, J., ... Xu, Y. Q. (2019). Improving the taste of autumn green tea with tannase. *Food Chemistry*, 277, 432–437. <https://doi.org/10.1016/j.foodchem.2018.10.146>
- Chen, Y., Chen, J., Chen, R., Xiao, L., Wu, X., Hu, L., ... Xiao, Y. (2022). Comparison of the fungal community, chemical composition, antioxidant activity, and taste characteristics of Fu brick tea in different regions of China. *Frontiers in Nutrition*, 9, 900138. <https://doi.org/10.3389/fnut.2022.900138>
- Chen, Y., Wang, Y., Chen, J., Tang, H., Wang, C., Li, Z., & Xiao, Y. (2020). Bioprocessing of soybeans (*Glycine max* L.) by solid-state fermentation with *Eurotium cristatum* YL-1 improves total phenolic content, isoflavone aglycones, and antioxidant activity. *RSC Advances*, 10(29), 16928–16941. <https://doi.org/10.1039/c9ra10344a>
- Dai, W., Qi, D., Yang, T., Lv, H., Guo, L., Zhang, Y., ... Lin, Z. (2015). Nontargeted analysis using ultraperformance liquid chromatography–quadrupole time-of-flight mass spectrometry uncovers the effects of harvest season on the metabolites and taste quality of tea (*Camellia sinensis* L.). *Journal of Agricultural and Food Chemistry*, 63(44), 9869–9878. <https://doi.org/10.1021/acs.jafc.5b03967>
- Dong, X. Z., & Cai, M. Y. (2001). *Manual of identification of common bacterial systems*. Science press.
- Du, Y., Yang, W., Yang, C., & Yang, X. (2022). A comprehensive review on microbiome, aromas and flavors, chemical composition, nutrition and future prospects of Fuzhuan brick tea. *Trends in Food Science & Technology*, 119, 452–466. <https://doi.org/10.1016/j.tifs.2021.12.024>
- Dufresne, C. J., & Farnworth, E. R. (2001). A review of latest research findings on the health promotion properties of tea. *The Journal of Nutritional Biochemistry*, 12(7), 404–421. [https://doi.org/10.1016/S0955-2863\(01\)00155-3](https://doi.org/10.1016/S0955-2863(01)00155-3)
- Ho, C. T., Zheng, X., & Li, S. (2015). Tea aroma formation. *Food Science and Human Wellness*, 4(1), 9–27. <https://doi.org/10.1016/j.fshw.2015.04.001>
- Hu, S., He, C., Li, Y., Yu, Z., Chen, Y., Wang, Y., & Ni, D. (2021). The formation of aroma quality of dark tea during pile-fermentation based on multi-omics. *LWT - Food Science and Technology*, 147, Article 111491. <https://doi.org/10.1016/j.lwt.2021.111491>
- Li, J., Xu, R., Zong, L., Brake, J., Cheng, L., Wu, J., & Wu, X. (2021). Dynamic evolution and correlation between metabolites and microorganisms during manufacturing process and storage of Fu Brick Tea. *Metabolites*, 11(10), 703. <https://doi.org/10.3390/metabo11100703>
- Li, W., & Wang, T. (2021). Effect of solid-state fermentation with *Bacillus subtilis* lwo on the proteolysis and the antioxidative properties of chickpeas. *International Journal of Food Microbiology*, 338, Article 108988. <https://doi.org/10.1016/j.ijfoodmicro.2020.108988>
- Li, Q., Li, Y., Luo, Y., Xiao, L., Wang, K., Huang, J., & Liu, Z. (2020). Characterization of the key aroma compounds and microorganisms during the manufacturing process of Fu brick tea. *LWT-Food Science and Technology*, 127, Article 109355. <https://doi.org/10.1016/j.lwt.2020.109355>
- Li, Q., Li, Y., Luo, Y., Zhang, Y., Chen, Y., Lin, H., ... Liu, Z. (2019). Shifts in diversity and function of the bacterial community during the manufacture of Fu brick tea. *Food Microbiology*, 80, 70–76. <https://doi.org/10.1016/j.fm.2019.01.001>
- Liu, M., Xie, H., Ma, Y., Li, H., Li, C., Chen, L., ... Zhao, M. (2020). High performance liquid chromatography and metabolomics analysis of tannase metabolism of gallic acid and gallates in tea leaves. *Journal of Agricultural and Food Chemistry*, 68(17), 4946–4954. <https://doi.org/10.1021/acs.jafc.0c00513>
- Liu, Z., Bruins, M. E., Ni, L., & Vincken, J. P. (2018). Green and black tea phenolics: Bioavailability, transformation by colonic microbiota, and modulation of colonic microbiota. *Journal of Agricultural and Food Chemistry*, 66(32), 8469–8477. <https://doi.org/10.1021/acs.jafc.8b02233>
- Lv, S., Wu, Y., Li, C., Xu, Y., Liu, L., & Meng, Q. (2014). Comparative analysis of Pu-erh and Fuzhuan teas by fully automatic headspace solid-phase microextraction coupled with gas chromatography–mass spectrometry and chemometric methods. *Journal of Agricultural and Food Chemistry*, 62(8), 1810–1818. <https://doi.org/10.1021/jf405237u>
- Ma, W., Zhu, Y., Shi, J., Wang, J., Wang, M., Shao, C., Yan, H., Lin, Z., & Lv, H. (2021). Insight into the volatile profiles of four types of dark teas obtained from the same dark raw tea material. *Food Chemistry*, 346, Article 128906. <https://doi.org/10.1016/j.foodchem.2020.128906>
- Ma, W., Zhu, Y., Ma, S., Shi, J., Yan, H., Lin, Z., & Lv, H. (2023). Aroma characterisation of Liu-pao tea based on volatile fingerprint and aroma wheel using SBSE-GC-MS. *Food Chemistry*, 414, Article 135739. <https://doi.org/10.1016/j.foodchem.2023.135739>
- Pripdeevech, P., Moonggoot, S., Popleuchai, S., & Chukeatirote, E. (2014). Analysis of volatile constituents of fermented tea with *Bacillus subtilis* by SPME-GC-MS. *Chiang Mai Journal of Science*, 41(2), 395–402. <http://epg.science.cmu.ac.th/ejournal/>
- Qi, B., Zhang, Y., Ren, D., Qin, X., Wang, N., & Yang, X. (2023). Fu Brick Tea Alleviates Constipation via Regulating the Aquaporins-Mediated Water Transport System in Association with Gut Microbiota. *Journal of Agricultural and Food Chemistry*, 71(8), 3862–3875. <https://doi.org/10.1021/acs.jafc.2c07709>
- Shi, J., Zhu, Y., Zhang, Y., Lin, Z., & Lv, H. P. (2019). Volatile composition of Fu-brick tea and Pu-erh tea analyzed by comprehensive two-dimensional gas chromatography–time-of-flight mass spectrometry. *LWT-Food Science and Technology*, 103, 27–33. <https://doi.org/10.1016/j.lwt.2018.12.075>
- Su, D., He, J. J., Zhou, Y. Z., Li, Y. L., & Zhou, H. J. (2022). Aroma effects of key volatile compounds in Keemun black tea at different grades: HS-SPME-GC-MS, sensory evaluation, and chemometrics. *Food Chemistry*, 373, Article 131587. <https://doi.org/10.1016/j.foodchem.2021.131587>
- Tanaka, T., Umeki, H., Nagai, S., Shii, T., Matsuo, Y., & Kouno, I. (2012). Transformation of tea catechins and flavonoid glycosides by treatment with Japanese post-fermented tea acetone powder. *Food Chemistry*, 134(1), 276–281. <https://doi.org/10.1016/j.foodchem.2012.02.136>
- Tasaki, S., Nakayama, M., & Shoji, W. (2017). Morphologies of *Bacillus subtilis* communities responding to environmental variation. *Development, Growth & Differentiation*, 59(5), 369–378. <https://doi.org/10.1111/dgd.12383>
- Wang, Z., Ma, B., Ma, C., Zheng, C., Zhou, B., Guo, G., & Xia, T. (2021). Region identification of Xinyang Maojian tea using UHPLC-Q-TOF/MS-based metabolomics coupled with multivariate statistical analyses. *Journal of Food Science*, 86(5), 1681–1691. <https://doi.org/10.1111/1750-3841.15676>
- Xia, F., Hu, S., Zheng, X., Wang, M. W., Zhang, C. C., Wu, Z. N., & Sun, Y. J. (2022). New insights into metabolomics profile generation in fermented tea: The relevance of bacteria and metabolites in Fuzhuan brick tea. *Journal of the Science of Food and Agriculture*, 102(1), 350–359. <https://doi.org/10.1002/jsfa.11365>
- Xiang, L. M., Liu, Y. Q., Lai, X. F., Li, Q. H., Sun, L. L., Chen, W. P., ... Sun, S. L. (2018). Biochemical component analysis and antioxidant activities of different kinds of aged tea. *Modern Food Science and Technology*, 34(4), 56–62. <https://doi.org/10.13982/j.mfst.1673-9078.2018.04.010>
- Xiang, M., Chu, J., Cai, W., Ma, H., Zhu, W., Zhang, X., ... Liu, X. (2022). Microbial succession and interactions during the manufacture of Fu Brick Tea. *Frontiers in Microbiology*, 13, Article 892437. <https://doi.org/10.3389/fmicb.2022.892437>
- Xiao, Y., He, C., Chen, Y., Ho, C. T., Wu, X., Huang, Y., ... Liu, Z. (2022a). UPLC–QQ–MS/MS-based widely targeted metabolomic analysis reveals the effect of solid-state fermentation with *Eurotium cristatum* on the dynamic changes in the metabolite profile of dark tea. *Food Chemistry*, 378, Article 131999. <https://doi.org/10.1016/j.foodchem.2021.131999>
- Xiao, Y., Huang, Y., Chen, Y., Zhu, M., He, C., Li, Z., ... Liu, Z. (2022b). Characteristic fingerprints and change of volatile organic compounds of dark teas during solid-state fermentation with *Eurotium cristatum* by using HS-GC-IMS, HS-SPME-GC-MS, E-nose and sensory evaluation. *LWT-Food Science and Technology*, 169, Article 113925. <https://doi.org/10.1016/j.lwt.2022.113925>
- Xiao, Y., Huang, Y., Chen, Y., Xiao, L., Zhang, X., Yang, C., ... Wang, Y. (2022c). Discrimination and characterization of the volatile profiles of five Fu brick teas from different manufacturing regions by using HS-SPME/GC-MS and HS-GC-IMS. *Current Research in Food Science*, 5, 1788–1807. <https://doi.org/10.1016/j.crf.2022.09.024>
- Xiao, Y., Wu, X., Yao, X., Chen, Y., Ho, C. T., He, C., ... Wang, Y. (2021a). Metabolite profiling, antioxidant and  $\alpha$ -glucosidase inhibitory activities of buckwheat processed by solid-state fermentation with *Eurotium cristatum* YL-1. *Food Research International*, 143, Article 110262. <https://doi.org/10.1016/j.foodres.2021.110262>
- Xiao, Y., Li, M., Liu, Y., Xu, S., Zhong, K., Wu, Y., & Gao, H. (2021b). The effect of *Eurotium cristatum* (MF800948) fermentation on the quality of autumn green tea. *Food Chemistry*, 358, Article 129848. <https://doi.org/10.1016/j.foodchem.2021.129848>
- Xiao, Y., Rui, X., Xing, G., Wu, H., Li, W., Chen, X., ... Dong, M. (2015). Solid state fermentation with *Cordyceps militaris* SN-18 enhanced antioxidant capacity and DNA damage protective effect of oats (*Avena sativa* L.). *Journal of Functional Foods*, 16, 58–73. <https://doi.org/10.1016/j.jff.2015.04.032>
- Xu, Q., Sun, M., Ning, J., Fang, S., Ye, Z., Chen, J., & Fu, R. (2019). The core role of *Bacillus subtilis* and *Aspergillus fumigatus* in pile-fermentation processing of Qingzhuo Brick Tea. *Indian Journal of Microbiology*, 59, 288–294. <https://doi.org/10.1007/s12088-019-00802-4>

- Xu, A., Wang, Y., Wen, J., Liu, P., Liu, Z., & Li, Z. (2011). Fungal community associated with fermentation and storage of Fuzhuan brick-tea. *International Journal of Food Microbiology*, 146(1), 14–22. <https://doi.org/10.1016/j.ijfoodmicro.2011.01.024>
- Xu, J., Zhang, Y., Yan, F., Tang, Y., Yu, B., Chen, B., ... Chen, H. (2022). Monitoring Changes in the Volatile Compounds of Tea Made from Summer Tea Leaves by GC-IMS and HS-SPME-GC-MS. *Foods*, 12(1), 146. <https://doi.org/10.3390/foods12010146>
- Yun, J., Cui, C., Zhang, S., Zhu, J., Peng, C., Cai, H., ... Hou, R. (2021). Use of headspace GC/MS combined with chemometric analysis to identify the geographic origins of black tea. *Food Chemistry*, 360, Article 130033. <https://doi.org/10.1016/j.foodchem.2021.130033>
- Zhang, W., Cao, J., Li, Z., Li, Q., Lai, X., Sun, L., ... Lai, Z. (2021). HS-SPME and GC/MS volatile component analysis of Yinghong No. 9 dark tea during the pile fermentation process. *Food Chemistry*, 357, Article 129654. <https://doi.org/10.1016/j.foodchem.2021.129654>
- Zheng, X. Q., Li, Q. S., Xiang, L. P., & Liang, Y. R. (2016). Recent Advances in Volatiles of Teas. *Molecules*, 21(3), 338. <https://doi.org/10.3390/molecules21030338>
- Zhu, W., Fang, X., Wang, W., Xu, W., Chen, W., Wu, S., ... Wang, S. (2022). Aroma effects of critical volatile compounds during thermophilic bacteria pile-fermentation in dark tea using gas chromatography mass spectrometry and odor activity value. *Food Science and Technology*, 42, Article e87022. <https://doi.org/10.1590/fst.87022>
- Zhu, Y., Chen, J., Chen, X., Chen, D., & Deng, S. (2020). Use of relative odor activity value (ROAV) to link aroma profiles to volatile compounds: Application to fresh and dried eel (*Muraenesox cinereus*). *International Journal of Food Properties*, 23(1), 2257–2270. <https://doi.org/10.1080/10942912.2020.1856133>
- Zhou, X., Ge, B., Zhang, X., Wang, K., Zhou, C., & Fu, D. (2022). Metabolomics analysis reveals the effects of compound fuzhuan brick tea (CFBT) on regulating dyslipidemia and metabolic disorders in mice induced by high-fat diet. *Nutrients*, 14(6), 1128. <https://doi.org/10.3390/nu14061128>
- Zhu, M., Ouyang, J., Zhou, F., Zhao, C., Zhu, W., Liu, C., ... Liu, Z. (2023). Polysaccharides from Fu brick tea ameliorate obesity by modulating gut microbiota and gut microbiota-related short chain fatty acid and amino acid metabolism. *The Journal of Nutritional Biochemistry*, 118, Article 109356. <https://doi.org/10.1016/j.jnutbio.2023.109356>